forests

MDPI

Article

The Effect of Fuel Bed Edges on Fire Dynamics

Luis Reis [1,2,3,*], Jorge Raposo [1,3,4], Hugo Raposo [3] and André Rodrigues [4]

[1] Ci2—Smart Cities Research Center, Polytechnic Institute of Tomar (Abrantes Higher School of Technology), 2300-313 Tomar, Portugal
[2] ISEC Lisboa—Higher Institute of Education and Sciences, Alameda das Linhas de Torres 179, 1750-142 Lisbon, Portugal
[3] RCM2+—Research Centre in Asset Management and System Engineering, Polytechnic Institute of Coimbra, Rua Pedro Nunes, 3030-199 Coimbra, Portugal
[4] Department of Civil Protection, Faculty of Natural Sciences, Engineering and Technologies, Lusófona University, Porto Campus, Rua Augusto Rosa, 24, 4000-098 Porto, Portugal
* Correspondence: luis.duarte.reis@ipt.pt

Abstract

Wildfires are among the most frequent and destructive natural hazards in Europe, particularly in Portugal. They have severe impacts on forests, ecosystems, human health, and infrastructure, leading to substantial socio-economic losses due to firefighting efforts and post-fire recovery costs. Moreover, wildfires cause numerous casualties each year, highlighting the need for a deeper understanding of fire behaviour to support effective firefighting strategies and ensure the safety of both responders and communities. This study examines the influence of wind flow velocity variation on fire behaviour, both in the presence and absence of an edge wall in the fuel bed, aiming to replicate the characteristics of real wildfire fronts at a laboratory scale. Experimental tests were conducted at the Forest Fire Research Laboratory (LEIF) of the University of Coimbra using a shrub mixture, composed of *Ulex europaeus*, *Baccharis trimera*, and *Caralluma adscendens*, representing one of the most common fine fuels in Portuguese forested landscapes. This research provides novel insights by experimentally analyzing the combined effect of wind velocity variation and fuel bed edge presence on fire behaviour, paving the way for future comparisons with numerical simulations and real wildfire fronts. As expected, increasing wind velocity and the presence of fuel bed edges resulted in higher values of rate of spread, fireline intensity, and fire intensity.

Keywords: fire behaviour; edge walls; laboratory tests; fire spread; fire intensity; wildfires

Check for updates

Academic Editor: Palaiologos Palaiologou

Received: 14 November 2025
Revised: 28 December 2025
Accepted: 8 January 2026
Published: 16 January 2026

Copyright: © 2026 by the authors. Licensee MDPI, Basel, Switzerland. This article is an open access article distributed under the terms and conditions of the Creative Commons Attribution (CC BY) license.

1. Introduction

In recent decades, Portugal has experienced a significant increase in both the frequency and severity of wildfires, with the catastrophic events of 2017, 2022, and 2024 highlighting the persistent limitations in disaster preparedness and response capacity [1–3]. Over the past century, the extent of burned areas and the associated socio-economic impacts have shown a consistent upward trend [4].

Natural and technological disasters, such as wildfires, exhibit dynamic behaviour influenced by multiple variables, including wind velocity and direction, terrain slope, fuel type and properties, humidity, and temperature [5–8]. Understanding how each of these factors affects fire behaviour is essential for predicting wildfire dynamics under varying environmental conditions. Such knowledge is critical for developing effective

adaptation and control strategies during firefighting operations. A systematic study of these parameters is therefore fundamental to characterizing and anticipating wildfire behaviour.

The development of a fire is significantly shaped by whether it occurs in an open or confined environment. Although the progression in both cases can share similar dynamics, open-space fires are strongly influenced by the type and amount of fuel available, as well as by the energy released, since oxygen availability is virtually unrestricted. Under these conditions, meteorological factors play a decisive role in determining fire behaviour.

In contrast, fires occurring in confined spaces exhibit distinct characteristics, primarily due to the limited availability of oxygen and the accumulation of combustion gases within the enclosure. These conditions significantly increase the likelihood of flashover or even explosion.

According to Bishop [9] and Drysdale [10], during the initial stages of a fire in a confined space, the rate of pyrolysis and the corresponding energy release are governed primarily by the combustion of the fuel itself and are independent of the compartment boundaries. As the fire develops, however, a transition may occur from a fuel-controlled to a ventilation-controlled regime, mainly depending on the surface area of the combustible materials. These phenomena have been extensively investigated in several studies [11–13].

Fire dynamics studies how fires ignite, propagate, develop, and ultimately extinguish. To accurately characterize fire behaviour, it is essential to consider the interactions between heat transfer and fluid mechanics [14]. Understanding fire dynamics is essential for accurately predicting fire behaviour in real-world scenarios and ensuring the safety of both firefighters and the general public. Such knowledge supports the development of effective firefighting strategies and helps identify situations where direct intervention may be unsafe due to rapid fire spread and intense energy release. With the growing frequency and scale of forest fires, a deeper understanding of fire behaviour has become critical. The catastrophic wildfires of 2017 in Portugal, particularly those that occurred in Pedrógão Grande in June and during the October fire complex, illustrate the urgent need to improve our knowledge of fire dynamics to prevent similar tragedies in the future [1–3].

Fire behaviour can be classified into two main categories: Normal Fire Behaviour (NFB) and Extreme Fire Behaviour (EFB) [15–17]. Additionally, three primary groups of factors influence fire behaviour: fuel characteristics, topography, and weather conditions. Together, these elements constitute the well-established and scientifically recognized "*Fire Triangle*" concept [18]. For further details, see [15–17].

However, time is also a critical factor influencing fire behaviour. According to Viegas (2006) [5], fire behaviour is inherently unstable, as fires may exhibit different propagation characteristics even when the previously mentioned factors remain constant over time. To address this, Viegas (2006) [5] proposed a refinement of the classic Fire Triangle, introducing the concept of the "Square of Fire", which incorporates time as an additional dimension influencing fire behaviour.

The article focuses on the fire dynamics in the presence of edge walls, aiming to determine whether these edge walls enable a laboratory fire to more accurately replicate wildfire behaviour under field conditions compared to setups without fuel bed edges.

This study introduces an innovative laboratory-scale approach to replicate wildfire front dynamics by analyzing the combined effect of wind velocity variation and fuel bed edge presence, a topic that has received limited attention in other research.

It is important to note that this study investigates the influence of fuel bed edges, which limits the possibility of making direct comparisons with previous work. We hypothesize that the presence of fuel bed edges confines the energy released during combustion, leading to increased fire intensity and a more realistic representation of wildfire behaviour compared to setups without fuel bed edges.

2. Materials and Methods

2.1. Physical Problem

In this study, a single fire line (I_G) is assumed to spread over flat terrain, both with and without fuel bed edges, under the influence of wind flow. The fire line is positioned at the beginning of the fuel bed, as schematically illustrated in Figure 1. A Cartesian coordinate system ($O_oX_oY_oZ_o$) is adopted, with O_oZ_o perpendicular to the ground. The study area is defined by the points ABCD, while EFGH represents the fuel bed area (with fuel bed edges). Line EF is offset by 2 m along the O_oX_o axis. The fuel bed is covered with a uniform layer of forest fuel to ensure consistent surface fire spread.

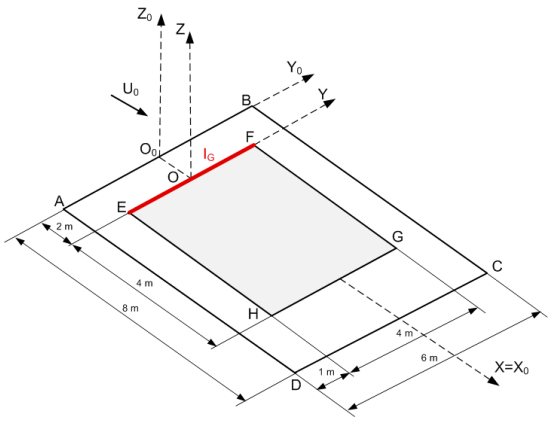


Figure 1. Geometry test used in the Forest Fire Research Laboratory (LEIF) of the University of Coimbra for tests without fuel bed edges.

The linear fire front, 4 m in length, is defined by the straight line I_G and is symmetric with respect to the OYZ plane. A uniform boundary-layer flow with a characteristic velocity (U_0) blows parallel to the OX_o axis, as indicated by the black arrows in Figure 1. At time t_0 = 0 s, the fire line is ignited and begins to spread along the OX plane.

This study was conducted at a laboratory scale, the physical principles of fire propagation remain equivalent to those observed in real fires: heat transfer by radiation and convection, flame tilt induced by wind, and combustion in fine fuel [19–21]. The experimental test was designed to maintain a continuous fire front, avoiding edge effects that could distort behaviour, as occurs in real wildfire fronts. This approach is consistent with studies comparing fire fronts from simulations and experimental tests, where representativeness depends on preserving dominant mechanisms rather than absolute scale, as described in the Fire Paradox project. Although a formal scale analysis based on dimensionless numbers was not performed, the mechanisms observed are compatible with those reported for surface fires under field conditions.

2.2. Experimental Study

Laboratory experiments were carried out in the Combustion Tunnel (wind-combustion tunnel) at the LEIF of the University of Coimbra (Portugal). The tunnel has a length of 8 m, a width of 6 m, and two side walls 2 m high, defined by points ABCD in Figure 1. The fuel bed area measured 4 × 4 m^2, with all sides equal to 4 m. To minimize boundary effects within the tunnel, a 2 m gap was maintained between the vertical walls of the combustion tunnel and the edges of the fuel bed (EF and GH). The tunnel is equipped with two 70 kW fans, capable of generating a flow velocity of up to 8 m/s.

Experimental tests were conducted under wind velocities of 0, 1, and 3 m/s.

The wind tunnel used in this study was previously characterized in published works [22], which report velocity profiles and turbulence parameters at the bed plane.

For free-stream velocities between 0–3 m/s, the boundary layer thickness above the bed is approximately 0.15–0.20 m, the turbulence intensity ranges from 2%–4%, and the integral scale is approximately 0.10 m. These values indicate an almost uniform flow with low turbulence, ensuring representative conditions for studying fire propagation.

The tests were monitored and recorded using an infrared camera (FLIR SC660) and two visible-range video cameras. For the infrared camera, the following parameters were applied: a temperature range of 300–1500 °C, an emissivity of 0.98 [23], and an acquisition rate of 15 Hz. A threshold of 350 °C was set to prevent obstruction of the view by the fire plume.

Both visible cameras were mounted on top of the lifting platform and operated in continuous recording mode. To minimize parallax errors, the angle between the infrared camera's optical axis and the combustion tunnel surface was approximately 90°. Infrared videos were used to determine the fire perimeter at predefined times, with the time interval between frames adjusted for each test to calculate the rate of spread (ROS).

One of the visible cameras was positioned laterally to provide an additional view, as recommended by Viegas (2006) [5]. Flame height measurements were obtained from images captured by this side camera, placed on the ground and perpendicular to the fire propagation line. For these recordings, a Sony FDR-AX100E camera was used.

The edge walls were constructed from autoclaved aerated concrete (Ytong, German brand) [24], composed of quartz sand, air, water, lime, cement, and aluminum powder. This material offers the following properties: fire resistance of up to 3 h, lightweight (approximately 75% lighter than conventional concrete), and high durability under normal weather conditions. Ytong was selected because its porosity is similar to that of the fuel bed, allowing the fire to propagate through it. The edge walls were built using Ytong aerated concrete blocks (dry density $\approx$ 550 kg/m^3). Based on the solid matrix density (~2600 kg/m^3), the estimated porosity is ~79%, consistent with manufacturer specifications. This porosity allows some air leakage; however, given the block thickness and typical permeability of aerated concrete (10^{-12}–10^{-13} m^2), the resulting seepage velocity under the tested pressure differences is negligible compared to the main airflow. Therefore, sidewall porosity does not significantly affect convective heat transfer.

Regarding radiative effects, Ytong is classified as Euroclass A1 (non-combustible) and has low thermal conductivity ($\leq$0.14 W/m K), which minimizes heat reflection and radiative feedback to the flames. Therefore, the influence of wall radiation on fire behaviour is considered negligible under the tested conditions.

The material properties are summarized in Table 1.

Table 1. Ytong Parameters [24].

Harmonized standard:	EN 771-4:2011+A1:2015 [25]
Reaction to fire	Euroclass A1, non-combustible
Gross dry bulk density, mean	550 [kg/m^3]
Water absorption—10 min/30 min/90 min	45/60/80 [g/(m^2·s$^{0.5}$)]
Water vapour diffusion coefficient, μ	5/10 [-] (Tabulated value according to EN 1745)
Thermal conductivity	λ_{10dry} (p = 50%) $\leq$ 0.14 [W/(m K)] λ_{10dry} (p = 90%) $\leq$ 0.14 [W/(m K)]

In each experiment, the fuel load and bulk density were carefully controlled, while laboratory conditions, including temperature (°C), relative humidity (%), and fuel moisture content (*mf*), were continuously monitored. The fuel bed consisted of a shrub mix-

ture [26,27], one of the most common fine fuels in Portuguese forests, with a specific fuel load of 1.5 kg/m^2 on a dry basis [28,29]. Fuel was evenly distributed across the tray using a manual procedure to ensure uniformity.

The fuel bed height (h_f) was measured at four random locations, with an average value of 18.7 cm and a variation within ±5 cm, confirming uniformity. The packing ratio (βf), defined as the ratio of the fuel bed bulk density (ρb) to the fuel particle density (ρp), was 0.029 [30–32]. The fuel properties were approximately as follows: particle surface-area-to-volume ratio (σf) 4734 m^{-1}; bulk density (ρb) 7.5 kg m^{-3}; fuel particle density (ρp) 258 kg m^{-3} and High Heat of Combustion (HHC) 18 kJ kg^{-1} [33,34]. The basic rate of spread (R_0, cm/s) of a linear fire front in a fuel bed with the same properties was determined for each series of tests using a 1 × 1 m^2 horizontal fuel bed, without slope or wind. The fire line was ignited by the same operator using a wool thread soaked in a mixture of petrol and diesel fuel.

The different configurations for each experimental test conducted in this study are summarized in Table 2. Each experiment was repeated three times under identical conditions to ensure reproducibility. For each variable (rate of spread, fire intensity, and flame height), the mean and standard deviation were calculated from these repetitions. Error bars shown in the figures represent the standard deviation of the measurements. Additionally, 95% confidence intervals were computed using Student's t-distribution and are reported in the tables to provide a measure of statistical reliability.

Table 2. Experimental Test Parameters.

Reference	Flow Velocity U (m/s)	Fuel Bed Edges	Average Moisture Content *mf* (%)	R_0 (cm/s)
Test 1	0	No	11.8	1.009
Test 2	1	No	10.6	
Test 3	3	No	12.7	
Test 4	0	Yes	12.4	
Test 5	1	Yes	12.1	
Test 6	3	Yes	12.6	

2.3. Evolution of ROS

The evaluation of the rate of spread (ROS) is measured using the position of the fire front along the axis OX; this means that, at a given instant, the position of the fire front is recorded after marking all the positions for each instant. If S_i and S_{i+1} represent the distances travelled by the fire front from the origin at the two consecutive time steps, the instantaneous value Rj of the ROS can be estimated using the following equation:

$$R_j = \frac{\Delta S_i}{\Delta t_i} = \frac{s_{i+1} - s_i}{t_{i+1} - t_i} \quad (1)$$

where t_i and t_{i+1} are the corresponding times for s_i and s_{i+1}.

The corresponding time t_j and distance S_j for this instantaneous value are given by:

$$t_j = \frac{t_i + t_{i+1}}{2} \quad (2)$$

$$S_j = \frac{s_i + s_{i+1}}{2} \quad (3)$$

As it is intended to correlate fire properties with R_j, the corresponding time tj will be determined for each time step.

To minimize the effect of the fuel moisture content *mf* and R_j, we reduce the rate of spread to nondimensional values [35]. Therefore, the nondimensional rate of spread (R′) is obtained using the R_0. As the equation shows.

$$R' = \frac{R_j}{R_0} \tag{4}$$

where R_0 is the basic ROS (cm/s), under no-slope and no-wind conditions.

The basic ROS R_0 is an intrinsic property of the fuel bed and depends mainly on the moisture content (*mf*) of the fuel particles [27,33,36,37].

For clarity, throughout this manuscript, the term "ROS" refers to the normalized rate of spread (R′), unless explicitly stated otherwise.

2.4. Fire Intensity

The most useful alternative to the real definition of fire intensity is the Byram's fire intensity, which is currently used as fireline intensity [38].

For this study we are first going to use the fireline intensity equation (Equation (5)) [18] to first determine the intensity of the fire for the centre point of the fire front profile, where *R* is the rate of spread, ΔHf is power of the fuel (in this case ΔHf = 20 MJ/kg), and *Wf* is the fuel load [39].

$$I_p = R \cdot \Delta H_f \cdot W_f \tag{5}$$

To have a better understanding of the fire behaviour when the two configurations (with and without fuel bed edges) are compared, we must resort to the fire intensity equation (Equation (6)) [39], where L_f is the flame length.

$$I_B = \left(\frac{L_f}{0.0775} \right)^{\frac{1}{0.46}} \tag{6}$$

2.5. Evolution of Flame Height and Tilt

Flame height was measured using images captured by a side-view camera (Sony FDR-AX100E) positioned on the floor and perpendicular to the fire propagation line. Video recordings were converted into frames using *Video to JPG Converter software V2.1.2*. To ensure comparable data across tests, frame extraction intervals were set at 20 s, 10 s, and 5 s for flow velocities of 0 m/s, 1 m/s, and 3 m/s, respectively.

Each extracted frame was analyzed to determine flame height and tilt using *Microsoft Office® 365 tools*. Measurements were taken for all frames and averaged to obtain the reported flame height values.

In addition to flame height, the angle of flame inclination was measured for each frame using the same image analysis procedure. The reported values correspond to the mean angle calculated across all frames for each test.

2.6. Statistical Analysis

Differences among flow velocities (U = 0, 1, 3 m/s) were assessed using simple linear regression for each response variable (fireline intensity: maximum and cumulative; rate of spread: maximum and cumulative; height of flame). We report 95% confidence intervals, t-statistics and coefficients of determination (R^2). The influence of fuel bed edges was evaluated using paired analyses at each flow velocity (Yes vs. No; *n* = 3 pairs), reporting mean differences, standard deviation, 95% confidence intervals, *p*-values, and paired effect

sizes (Cohen's dz). Normality of differences was checked using the Shapiro–Wilk test; when violated, Wilcoxon signed-rank tests were applied.

Additionally, Pearson correlations were computed to quantify associations among key fire behaviour variables (ROS, fire intensity, flame height) under different wind regimes, reporting r-values, 95% confidence intervals, and *p*-values.

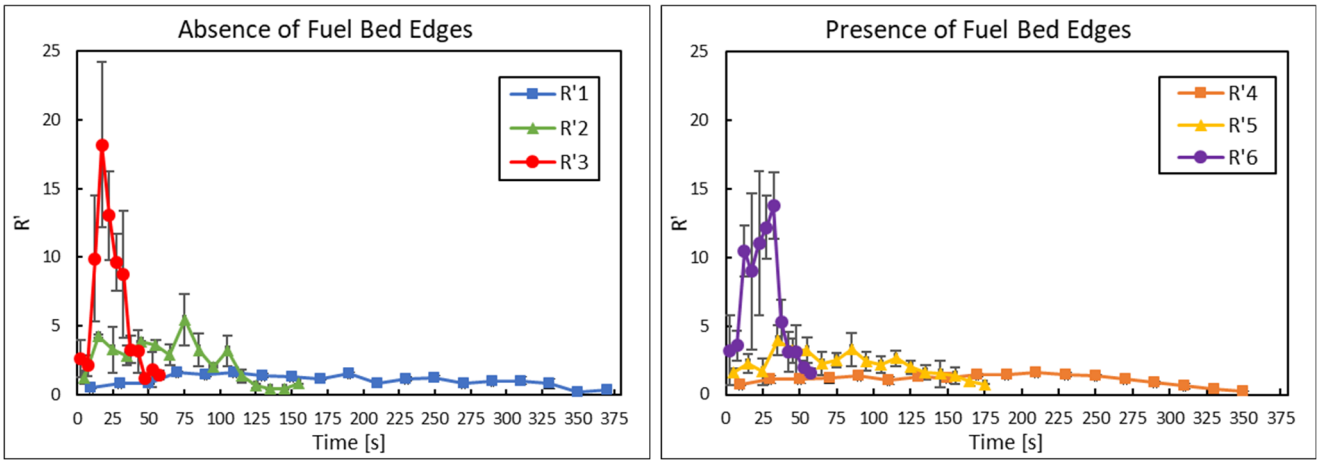
The significance level was set at $\alpha = 0.05$, and all analyses were conducted using *IBM SPSS Statistics* version 28.

3. Results

In each section, the variability of the measurements is represented by the error bars in the figures, which correspond to the standard deviation of the repeated tests. Additionally, 95% confidence intervals for the main variables (ROS, fire intensity, flame height and flame tilt) are provided in Tables 3, 4, 5 and 6, respectively. These intervals provide a clearer representation of the uncertainty associated with the measurements and improve the interpretation of the results.

3.1. Evolution of Normalized Rate of Spread (R′)

The evolution of the normalized rate of spread (R′) for different flow velocities (Figure 2) was recorded using an infrared camera, and the captured frames were subsequently analyzed to determine the R′. For this analysis, normalized rate of spread values from all experimental tests were compiled and grouped according to the corresponding flow velocities (0, 1, and 3 m/s). The series R′1, R′2, R′3, R′4, R′5, and R′6 represent the average ROS values for each respective experiment.



(**a**) (**b**)

Figure 2. Normalized rate of spread (R′) for different flow velocities (0, 1 and 3 m/s) (**a**) with and (**b**) without the presence of fuel bed edges.

The influence of flow velocity on the rate of spread increases with higher wind speeds. This observation aligns with the hypothesis that the ROS significantly increases when the wind direction is aligned with the direction of fire propagation [5].

The rate of spread exhibits considerable fluctuations in a fuel bed without edges, showing highly variable values at successive time steps for the same flow velocity. The figure indicates that, for flow velocities greater than 0 m/s, the ROS peaks near the mid-length of the fuel bed tray. However, rate of spread oscillations are noticeably smaller when fuel bed edges are present.

Normalized rate of spread (R′) increased significantly with wind speed (linear regression, $p < 0.001$), with the largest effect observed between 1 m/s and 3 m/s. At U = 0 m/s,

propagation was minimal, while at U = 3 m/s, mean R′ values were up to 5 times higher than baseline (U = 0 m/s).

The 95% confidence intervals were calculated using Student's t-distribution and are presented in Table 3 for the normalized rate of spread in each test.

Table 3. Estimated normalized rate of spread (R′) and 95% Confidence Intervals for all tests.

Instant Measure	R′1	R′2	R′3	R′4	R′5	R′6
1	0.53 ± 0.29	1.28 ± 1.16	2.64 ± 3.35	0.72 ± 0.13	1.63 ± 0.69	3.22 ± 6.32
2	0.81 ± 0.73	4.24 ± 0.32	2.12 ± 1.9	1.11 ± 0.66	2.24 ± 1.74	3.56 ± 2.68
3	0.85 ± 0.07	3.29 ± 4.14	9.88 ± 11.38	1.1 ± 0.76	1.68 ± 2.38	10.47 ± 4.67
4	1.64 ± 0.27	2.85 ± 1.8	18.19 ± 15.01	1.2 ± 0.92	3.96 ± 2.81	8.99 ± 14.17
5	1.46 ± 0.38	3.88 ± 0.16	13.02 ± 7.94	1.34 ± 0.07	3.22 ± 2.24	11.05 ± 13.02
6	1.6 ± 0.7	3.6 ± 0.9	9.63 ± 5.19	1.04 ± 0.71	3.25 ± 2.3	12.18 ± 5.7
7	1.39 ± 0.33	2.92 ± 1.87	8.78 ± 11.45	1.31 ± 0.76	2.28 ± 2.07	13.76 ± 6.01
8	1.33 ± 0.38	5.46 ± 4.61	3.3 ± 2.45	1.21 ± 0.31	2.54 ± 1.3	5.29 ± 4
9	1.19 ± 0.2	3.26 ± 3.02	3.16 ± 3.91	1.42 ± 0.35	3.28 ± 3.03	3.14 ± 3.64
10	1.54 ± 0.33	2.05 ± 0.18	1.16 ± 0.64	1.42 ± 0.42	2.41 ± 1.73	3.1 ± 4.81
11	0.88 ± 0.16	3.19 ± 2.76	1.86 ± 3.18	1.61 ± 0.09	2.16 ± 1.53	1.96 ± 1.29
12	1.15 ± 0.36	1.36 ± 1.11	1.43 ± 0.81	1.46 ± 0.36	2.63 ± 1.42	1.62 ± 0.7
13	1.27 ± 0.3	0.65 ± 0.37		1.39 ± 0.08	1.99 ± 1.19	
14	0.81 ± 0.71	0.45 ± 0.05		1.12 ± 0.17	1.63 ± 1.26	
15	0.97 ± 0.03	0.44 ± 0.02		0.86 ± 0.26	1.53 ± 2.41	
16	1.03 ± 0.64	0.82 ± 0.03		0.62 ± 0.44	1.38 ± 1.48	
17	0.82 ± 0.85			0.41 ± 0.47	0.98 ± 0.86	
18	0.19 ± 0.12			0.25 ± 0.03	0.74 ± 0.03	
19	0.34 ± 0.02					

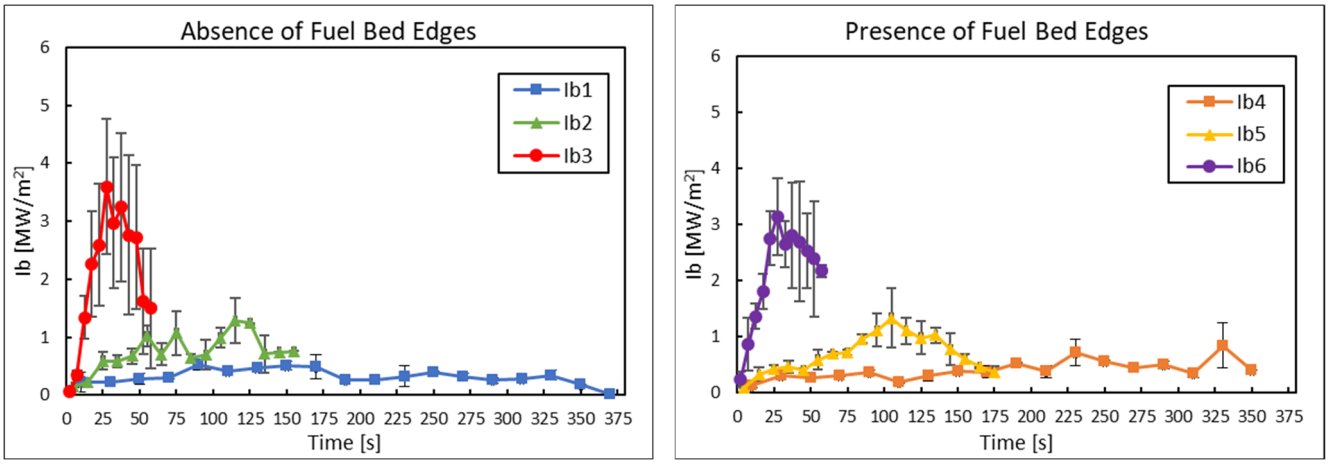
3.2. Evolution of Fire Intensity

The fire intensity values were calculated based on the previously determined flame length, using Equation (6). For this analysis, the fire intensity values [MW/m^2] from all experimental tests were compiled and grouped according to the corresponding flow velocities (0, 1, and 3 m/s). The series Ib1, Ib2, Ib3, Ib4, Ib5 and Ib6 represent the average fire intensity values for each respective experiment. The fire intensity for each flow velocity is shown in Figure 3.

The results indicate that the rate of spread and fire intensity are generally lower in tests with fuel bed edges compared to those without edges. Although experiments without fuel bed edges exhibited higher peak values, the cumulative fireline intensity was greater in the tests performed with fuel bed edges.

Maximum fire intensity showed a significant positive association with wind speed ($p < 0.001$), while edge walls had no significant effect ($p > 0.05$).

The 95% confidence intervals were calculated using Student's t-distribution and are presented in Table 4 for the fire intensity in each test.



(**a**) (**b**)

Figure 3. Fire Intensity for different flow velocities (0, 1 and 3 m/s) (**a**) with and (**b**) without the presence of fuel bed edges.

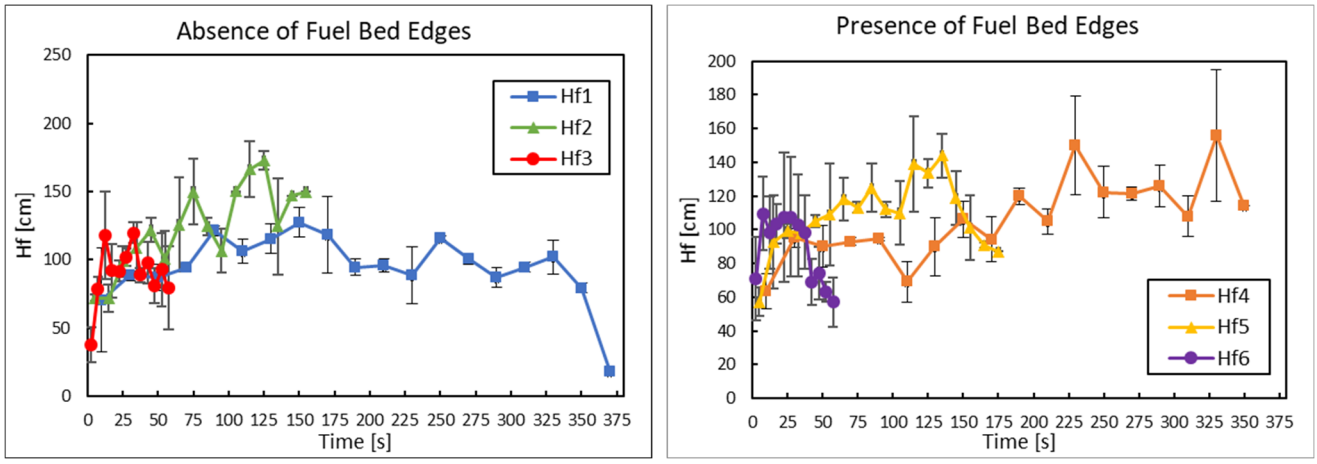
Table 4. Estimated Fire Intensity and 95% Confidence Intervals for all tests.

Instant Measure	Ib1	Ib2	Ib3	Ib4	Ib5	Ib6
1	0.22 ± 0.42	0.15 ± 0	0.06 ± 0.1	0.13 ± 0.07	0.1 ± 0.04	0.24 ± 0.35
2	0.23 ± 0.02	0.22 ± 0.03	0.34 ± 0.2	0.31 ± 0.12	0.33 ± 0.31	0.86 ± 1.17
3	0.29 ± 0.24	0.59 ± 0.39	1.34 ± 0.92	0.28 ± 0.12	0.42 ± 0.17	1.36 ± 0.55
4	0.31 ± 0.05	0.59 ± 0.26	2.27 ± 2.25	0.31 ± 0	0.46 ± 0.27	1.81 ± 0.78
5	0.53 ± 0.2	0.68 ± 0.32	2.6 ± 2.62	0.37 ± 0.12	0.4 ± 0.08	2.75 ± 1.2
6	0.42 ± 0.13	1.02 ± 0.45	3.6 ± 2.91	0.19 ± 0.03	0.59 ± 0.43	3.14 ± 1.7
7	0.46 ± 0.11	0.71 ± 0.47	2.97 ± 2.8	0.31 ± 0.25	0.71 ± 0.07	2.66 ± 1.02
8	0.51 ± 0.19	1.08 ± 0.94	3.24 ± 3.16	0.39 ± 0.13	0.72 ± 0.11	2.8 ± 2.33
9	0.49 ± 0.51	0.63 ± 0.21	2.76 ± 3.41	0.38 ± 0.26	0.96 ± 0.21	2.69 ± 2.64
10	0.27 ± 0.06	0.7 ± 0.63	2.72 ± 3.09	0.53 ± 0.01	1.11 ± 0.73	2.53 ± 1.65
11	0.27 ± 0.08	0.99 ± 0.42	1.62 ± 2.25	0.38 ± 0.26	1.33 ± 1.3	2.39 ± 2.54
12	0.33 ± 0.43	1.29 ± 0.97	1.5 ± 2.56	0.72 ± 0.6	1.11 ± 0.58	2.18 ± 0.27
13	0.4 ± 0.03	1.24 ± 0.01		0.56 ± 0.04	0.99 ± 0.75	
14	0.33 ± 0.12	0.72 ± 0.8		0.45 ± 0.02	1.03 ± 0.35	
15	0.26 ± 0.11	0.75 ± 0.01		0.5 ± 0.16	0.78 ± 0.68	
16	0.28 ± 0.07	0.76 ± 0.01		0.35 ± 0.19	0.6 ± 0.23	
17	0.35 ± 0.21			0.85 ± 1	0.46 ± 0.01	
18	0.19 ± 0.02			0.4 ± 0.01	0.38 ± 0.25	
19	0.01 ± 0.01					

3.3. Evolution of Flame Height

The flame height is a key parameter in fire characterization, as it allows the estimation of the flame length when combined with the flame tilt angle, as explained later. The variation in flame height for each flow velocity is shown in Figure 4. For this analysis, the flame height values from all experimental tests were compiled and grouped according to

the corresponding flow velocities (0, 1, and 3 m/s). The series Hf1, Hf2, and Hf3 represent the average flame height values for each respective experiment.



(**a**) (**b**)

Figure 4. Flame height for different flow velocities (0, 1 and 3 m/s) (**a**) with and (**b**) without the presence of fuel bed edges.

The figure reveals an interesting observation: for a flow velocity of 0 m/s, flame height exhibits only minor fluctuations compared to those recorded at higher flow velocities. Additionally, for a flow velocity of 3 m/s, flame height does not reach the same magnitude as at 1 m/s, since the fire front reaches the end of the fuel bed more rapidly, limiting flame growth due to the depletion of available fuel.

When fuel bed edges are present, flame height shows very similar values for all flow velocities, indicating that the flame height is more stable under these conditions. This also suggests that, as expected, flame tilt angles increase with wind speed, as observed in the experiments without fuel bed edges, resulting in greater flame lengths at higher wind velocities.

The 95% confidence intervals were calculated using Student's t-distribution and are presented in Table 5 for the flame height in each test.

Table 5. Estimated Flame Height and 95% Confidence Intervals for all tests.

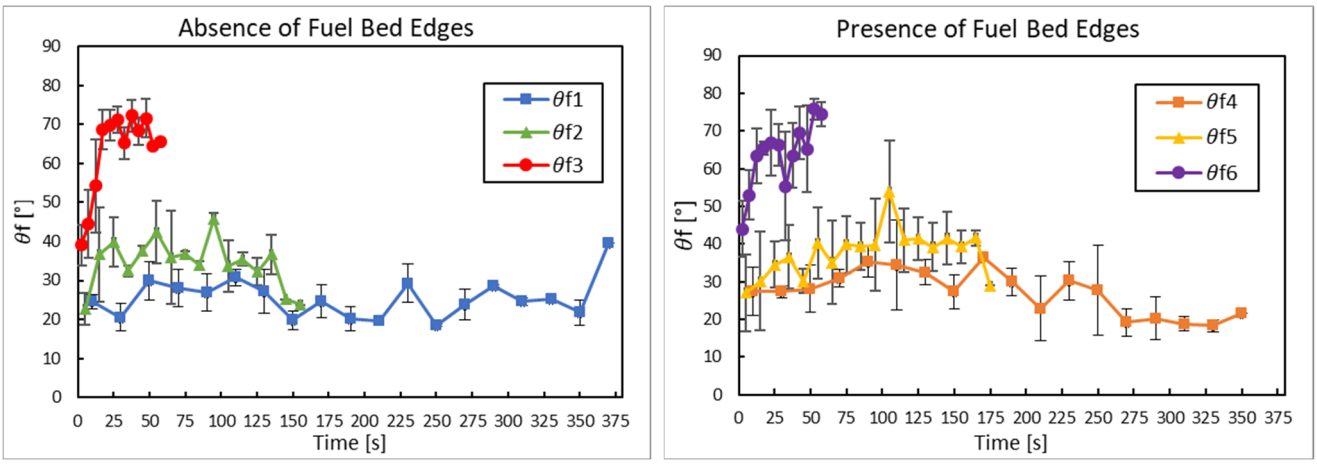
Instant Measure	Hf1	Hf2	Hf3	Hf4	Hf5	Hf6
1	70.5 ± 94.32	72 ± 6.09	37.65 ± 31.89	63.75 ± 25.86	57.25 ± 21.49	70.99 ± 61.74
2	88.5 ± 9.13	72 ± 24.34	78.5 ± 21.62	95.25 ± 13.69	92.95 ± 69.07	109.65 ± 53.6
3	87.15 ± 24.65	98.78 ± 27.54	118.1 ± 79.03	90 ± 30.43	99 ± 10.54	98.33 ± 52.93
4	94.5 ± 3.04	108.75 ± 47.16	91.95 ± 47.87	93 ± 6.09	98 ± 8.05	103.54 ± 29.2
5	121.5 ± 9.13	121.88 ± 22.06	91.65 ± 18.9	94.5 ± 3.04	105 ± 9.13	107.51 ± 95.7
6	106.5 ± 21.3	100.5 ± 51.73	102 ± 15.81	69.23 ± 29.97	108.95 ± 74.8	107.59 ± 88.06
7	115.5 ± 27.38	126 ± 85.2	120 ± 18.26	90 ± 42.6	118 ± 31.77	102.56 ± 75.78
8	127.58 ± 27.23	150.08 ± 60.7	89 ± 13.26	106.28 ± 26.93	113 ± 8.05	98.55 ± 53.73
9	118.5 ± 69.98	124.5 ± 15.21	98 ± 37.39	94.35 ± 33.17	124.85 ± 35.19	68.96 ± 33.96

Table 5. *Cont.*

Instant Measure	Hf1	Hf2	Hf3	Hf4	Hf5	Hf6
10	94.5 ± 15.21	106.5 ± 39.55	80.8 ± 31.88	120 ± 12.17	112 ± 10.97	74.25 ± 38.98
11	96 ± 12.17	150.15 ± 0.3	93 ± 66.94	105 ± 18.26	110 ± 47.24	63.2 ± 14.15
12	88.65 ± 52.03	166.65 ± 51.42	79.5 ± 76.07	150.15 ± 72.72	139.1 ± 70.13	57.15 ± 36.82
13	116.1 ± 4.26	173.03 ± 16.58		122.18 ± 38.19	133.55 ± 20.48	
14	100.5 ± 9.13	124.5 ± 88.24		121.5 ± 9.13	143.95 ± 32.95	
15	87 ± 18.26	147 ± 0.2		126 ± 30.43	119 ± 39.9	
16	94.5 ± 9.13	150 ± 0.1		108 ± 30.43	101.25 ± 47.92	
17	102 ± 30.43			156 ± 97.37	90.75 ± 4.56	
18	79.43 ± 9.28			114 ± 0.2	87 ± 0.1	
19	18 ± 0.2					

3.4. Evolution of Flame Tilt

The flame tilt is defined as the angle between the flame axis and the vertical. Figure 5 presents the results of each test. These values, as well as flame height, were obtained from side-view images captured during the experiments.



(**a**) (**b**)

Figure 5. Flame tilt for different flow velocities (0, 1 and 3 m/s) (**a**) with and (**b**) without the presence of fuel bed edges.

Flame tilt measurements from all tests were compiled and grouped according to the corresponding flow velocities (0, 1, and 3 m/s). The series represents the average flame tilt for each respective experiment.

Analysis of the figure shows that, without wind, flame tilt remains nearly constant, confirming that flames exhibit an almost vertical profile under no-flow conditions. Flame height increased significantly with wind speed ($p < 0.001$), and edge walls significantly reduced flame height at U = 1 m/s ($p = 0.025$), but had no effect at higher speeds.

The 95% confidence intervals were calculated using Student's t-distribution and are presented in Table 6 for the flame tilt in each test.

Table 6. Estimated Flame Tilt and 95% Confidence Intervals for all tests.

Instant Measure	θf1	θf2	θf3	θf4	θf5	θf6
1	24.58 ± 4.61	22.7 ± 10.05	39.03 ± 12.9	27.33 ± 16	27.07 ± 25.26	43.91 ± 18.46
2	20.5 ± 8.75	36.66 ± 29.78	44.46 ± 21.73	27.29 ± 4.01	30.12 ± 32.4	52.97 ± 16.19
3	29.9 ± 12.27	39.91 ± 15.59	54.25 ± 29.88	28.14 ± 15.6	34.49 ± 15.27	63.3 ± 17.94
4	28.04 ± 12.19	32.53 ± 3.48	68.67 ± 12.68	30.87 ± 5.86	36.51 ± 21.01	65.45 ± 4.53
5	26.91 ± 11.91	37.67 ± 3.04	69.74 ± 9.97	35.21 ± 10.14	30.15 ± 7.86	66.91 ± 21.65
6	30.73 ± 5.04	42.37 ± 19.78	71.2 ± 8.48	34.42 ± 29.77	40.26 ± 23.53	66.26 ± 13.93
7	27.24 ± 13.86	35.99 ± 29.58	65.18 ± 9.88	32.46 ± 8.13	35.11 ± 27.7	55.34 ± 35.85
8	19.75 ± 6.19	36.67 ± 1.64	72.26 ± 10.17	27.38 ± 11.17	39.85 ± 18.86	63.47 ± 21.23
9	24.62 ± 10.4	33.96 ± 2.63	68.26 ± 8.87	36.43 ± 2.45	39.31 ± 15.33	69.55 ± 17.42
10	20.15 ± 7.94	45.82 ± 3.61	71.53 ± 12.19	29.98 ± 9.04	39.78 ± 30.14	65.26 ± 28.89
11	19.69 ± 2.36	33.77 ± 16.49	64.37 ± 0.76	22.84 ± 21.3	53.81 ± 33.61	75.84 ± 6.84
12	29.29 ± 12.35	35.4 ± 4.14	65.5 ± 2.65	30.31 ± 12.71	41.02 ± 20.79	74.44 ± 7.92
13	18.51 ± 0.63	32.32 ± 8.94		27.83 ± 29.62	41.38 ± 13.94	
14	23.8 ± 9.64	36.65 ± 12.46		19.15 ± 8.94	39.18 ± 16.01	
15	28.61 ± 0.58	25.14 ± 0.82		20.24 ± 14.21	41.5 ± 17.23	
16	24.61 ± 2.55	23.7 ± 0.51		18.81 ± 4.93	39.3 ± 10.93	
17	25.26 ± 0.87			18.28 ± 3.76	41.57 ± 4.95	
18	21.8 ± 8.07			21.54 ± 0.42	28.89 ± 0.66	
19	39.52 ± 0.55					

4. Discussion

The potential influence of turbulence induced by the boundary walls was considered. The experimental setup included lateral walls that could affect airflow patterns, particularly near the edges of the fuel bed. However, the analysis of flame tilt and height in regions close to and away from the walls (Figures 4a,b and 5a,b) indicates that the effect of wall-induced turbulence was minimal under the tested conditions. Despite the presence of boundary walls, no substantial changes in flame tilt and height were observed up to 3 m/s, suggesting a regime where radiation predominates over convection in flat geometries and beds of moderate width. Studies with more confined geometries and/or slopes show clear transitions to plume adhesion and upstream convective heating, with marked increases in rate of spread and flame length (e.g., fuel bed width and walls in [40], and flow visualizations in [41]).

Although this study was conducted at a laboratory scale, the observed values are consistent with those reported for grassland fires under similar wind conditions. For example, the maximum rate of spread measured (≈0.18 m/s) and fireline intensity (up to 3.98 MW/m) fall within the range documented for surface fires under moderate wind speeds (rate of spread typically 0.1–0.5 m/s, intensity 0.5–3 MW/m) [42,43]. Flame heights observed in our tests (up to ~0.8 m) also align with field observations for comparable fuel loads. These similarities indicate that, despite scale differences, the dominant physical mechanisms, radiation and convection, flame tilt under wind are preserved, supporting the representativeness of the experimental setup.

The maximum and cumulative values of the normalized rate of spread and fireline intensity were also analyzed for each experiment. This approach enables the assessment of whether the presence of fuel bed edges effectively leads to higher R′ and fireline intensity values. The maximum and cumulative results for these parameters are summarized in Table 7.

Table 7. Comparison of peak and cumulative values of normalized rate of spread (R′) and Fireline Intensity for optimized measurements.

Reference	Fireline Intensity [MW/m]		Normalized Rate of Spread [m/s]		Flow Velocity U (m/s)	Fuel Bed Edges
	Maximum Value	Cum	Maximum Value	Cum		
Experiment 1	0.42	5.25	1.39	17.51	0	No
Experiment 2	1.15	10.52	3.82	35.08	1	No
Experiment 3	3.40	20.80	11.34	69.32	3	No
Experiment 4	0.47	5.83	1.56	19.43	0	Yes
Experiment 5	1.17	11.62	3.88	38.73	1	Yes
Experiment 6	3.98	22.86	13.28	76.21	3	Yes

Analysis of the data presented in Table 7 indicates that the rate of spread is higher when fuel bed edges are present. This observation is supported by the corresponding increase in fire intensity, as tests with fuel bed edges consistently exhibited higher intensity values. According to Byram [18], greater fire intensity implies a higher rate of spread, which reinforces this result. These findings suggest that fuel bed edges provide a preferential pathway for flame propagation, promoting faster and more uniform fire spread due to the more linear fire front profile.

The observed increase in rate of spread near fuel bed edges can be attributed to enhanced airflow and heat transfer at the boundaries, which accelerates combustion. The increase in rate of spread and fireline intensity in the presence of edges suggests flow channelling and more efficient heating of adjacent fuels, producing more linear and uniform fire fronts. involving bed width and boundary walls showed similar trends, with increases in rate of spread, flame height, and flame length, and a transition from radiation-dominated to convection-dominated regimes as the geometry favours plume adhesion [40]. In porous beds, heat flux measurements indicate that the structure can enhance local heating, consistent with the effect observed near the edges [44]. Conversely, for very wide fire fronts, radiative gain tends to saturate [45], framing the role of edges as enhancers of convective efficiency rather than global radiation.

All variables showed strong positive associations with flow velocity (U). Linear regression yielded significant slopes: fireline intensity (maximum) b = 1.108 MW/m·(95% CI: 0.842–1.374; R^2 = 0.971, $p < 0.001$), fireline intensity (cumulative) b = 5.423 (4.648–6.198; R^2 = 0.990; $p < 0.001$), ROS (maximum) b = 3.700 (2.807–4.593; R^2 = 0.971; $p < 0.001$), and cumulative ROS b = 18.074 (15.490–20.660; R^2 = 0.989; $p < 0.001$). The strong positive dependence of all variables on U is consistent with empirical wind-assisted models [42,43], and reflects the increase in flame tilt and convective heat transfer to unburned fuel.

The literature on the trench effect indicates that the presence of walls or slopes can induce plume adhesion and convective coupling [46,47], mechanisms that help explain the increase in ROS observed near edges, even on flat terrain.

Paired comparisons based on wind speed show that, at U = 1 m/s, edge walls significantly reduce the average flame height (difference = 13.53 cm, 95% CI [1.90, 25.15],

p = 0.025), without altering the mean ROS or fireline intensity. At U = 0 and U = 3 m/s, no systematic mean effects of barriers were detected (95% CI includes 0), although paired correlations between metrics with and without barriers were moderate to strong (e.g., ROS at U = 3 m/s: r ≈ 0.78, p ≈ 0.0025), indicating high consistency of behaviour under the same wind regime. These results suggest a real geometric effect of barriers in moderate wind conditions, while in strong winds, behaviour is predominantly controlled by the wind conditions, in agreement with studies on radiation–convection transitions and the influence of geometry [40,41].

Comparison with Other Studies

The results obtained show that the presence of fuel bed edges is associated with increases in ROS and fireline intensity (Table 6), consistent with a scenario of flow channelling and more effective convective heating near the boundaries. Controlled tests involving boundary walls and variation in fuel bed width have reported similar trends, showing increases in ROS, flame height, and flame length with increasing width and slope, along with a regime transition in which convection becomes dominant over radiation when the plume adheres to the surface [40].

Flow visualization studies indicate that plume or flame adhesion results from an imbalance between entrainment and pressure gradients, which drive hot gases uphill or along confined surfaces, thereby reinforcing the heating potential of upstream fuel [48].

In the context of trench geometries, the literature on the trench effect documents sudden accelerations and extremes of behaviours when the flame adhesion occurs and convective coupling intensifies [41,46], providing a conceptual framework that helps interpret the increase in ROS observed at the edges, even on flat surfaces.

The role of bed structure and height has been highlighted in both field and laboratory studies: reductions in height tend to decrease ROS [48], while heat flux measurements demonstrate that porous structures can dominate heating under windless conditions [44]. These results support the view that fuel geometry and structure strongly influence transfer mechanisms and, consequently, ROS.

The strong dependence of ROS and fireline intensity on flow velocity (U) observed in the regressions is consistent with empirical wind-assisted models and field studies in grassland [42,43], reinforcing that wind tilts the flame and intensifies convective heat transfer to unburned fuel.

Our results show that edges and geometric parameters (width, structure) shape heat transfer mechanisms, promoting more linear fire fronts and higher ROS under certain conditions, in qualitative agreement with the referenced studies. However, more pronounced transitions to full plume adhesion and convection typically occur on slopes or in more confined geometries (e.g., critical angles of approximately 20°).

5. Conclusions

This study investigated the effect of fuel bed edges on fire dynamics in a wind tunnel, with the main goal of understanding how these edges influence fire behaviour and whether their presence can reproduce more realistic fire conditions. Two key factors known to affect fire behaviour were analyzed: flow velocity and the presence of fuel bed edges.

As the flow velocity increased, all analyzed fire parameters, such as the rate of spread and fire intensity, also increased, since the wind direction was aligned with the direction of fire propagation. In the case of the fuel bed edges, it was initially expected that these parameters would also increase, as the edges provide a defined path for the fire to follow. However, preliminary analyses did not confirm this hypothesis.

After performing additional optimized measurements, it was found that the inclusion of fuel bed edges led to higher values for all analyzed parameters compared with the tests without edges. The comparison of all experimental results confirms that the presence of fuel bed edges promotes more intense fire behaviour, characterized by higher rates of spread and greater fire and fireline intensities.

These findings suggest that incorporating fuel bed edges contributes to reproducing a fire behaviour that more closely resembles that of real forest fires.

This study has some limitations that should be considered. The tests were conducted in a laboratory, which implies simplifications in relation to actual field conditions, such as terrain heterogeneity and fuel variability. In addition, the geometry used was predominantly flat and moderately confined, not covering scenarios with steep slopes or extreme confinement, in which the transition to convection-dominated regimes may occur more pronouncedly. The study considered a single type of fuel with homogeneous characteristics, not including structural or moisture variations that can significantly influence heat transfer mechanisms and propagation rates. Despite these limitations, the results obtained are consistent with field studies and provide a solid basis for future investigations on larger scales and under more complex conditions.

Author Contributions: Conceptualization, L.R. and J.R.; methodology, L.R.; validation, L.R. and J.R.; formal analysis, L.R.; data curation, L.R.; writing—original draft preparation, L.R.; writing—review and editing, L.R., H.R. and A.R. All authors have read and agreed to the published version of the manuscript.

Funding: This article was supported by FCT—Fundação para a Ciência e a Tecnologia, under the project "Centro de Investigação em Cidades Inteligentes" (reference UID/05567/2025), which has been assigned the DOI: https://doi.org/10.54499/UID/05567/2025. The authors acknowledge the Forest Fire Research Laboratory (LEIF) of the Forest Fire Research Center (CEIF) of ADAI, University of Coimbra (UC), for their support required for the development of the tests.

Data Availability Statement: Data are available only under request to the corresponding author: Luís Reis, luis.duarte.reis@ipt.pt.

Conflicts of Interest: The authors declare no conflicts of interest.

Abbreviations

The following abbreviations are used in this manuscript:

ΔHf	Power of the fuel [MJ/kg]
h_f	Fuel bed height [cm]
βf	Packing ratio
ρb	Fuel bed bulk density
ρp	Fuel particle density
σf	Particle surface-area-to-volume ratio
Ib	Fire intensity [MW/m^2]
L_f	Flame length [m]
mf	Fuel moisture content [%]
NFB	Normal Fire Behaviour
R_0	Basic rate of spread [cm/s]
R′	Nondimensional rate of spread
ROS	Rate of spread [m/s]
S	Distances travelled by the fire line from the origin
U	Flow Velocity [m/s]
Wf	Fuel load [kg/m^2]

References

1. Comissão Técnica Independente Análise e Apuramento dos Factos Relativos aos Incêndios que Ocorreram em Pedrogão Grande. Available online: https://www.parlamento.pt/ArquivoDocumentacao/Documents/Incendios_Junho%202017_Relatorio.pdf (accessed on 28 December 2025).
2. Domingos Xavier Viegas O complexo de Incêndios de Pedrógão Grande e Concelhos Limítrofes, Iniciado a 17 de Junho de 2017. Available online: https://www.portugal.gov.pt/pt/gc21/comunicacao/documento?i=o-complexo-de-incendios-de-pedrogao-grande-e-concelhos-limitrofes-iniciado-a-17-de-junho-de-2017 (accessed on 28 December 2025).
3. Domingos Xavier Viegas Análise dos Incêndios Florestais Ocorridos a 15 de Outubro de 2017. Available online: https://www.portugal.gov.pt/pt/gc21/comunicacao/documento?i=analise-dos-incendios-florestais-ocorridos-a-15-de-outubro-de-2017 (accessed on 28 December 2025).
4. Moreira, F.; Viedma, O.; Arianoutsou, M.; Curt, T.; Koutsias, N.; Rigolot, E.; Barbati, A.; Corona, P.; Vaz, P.; Xanthopoulos, G.; et al. Landscape—Wildfire interactions in southern Europe: Implications for landscape management. *J. Environ. Manag.* **2011**, *92*, 2389–2402. [CrossRef]
5. Viegas, D.X. Parametric study of an eruptive fire behaviour model. *Int. J. Wildland Fire* **2006**, *15*, 169–177. [CrossRef]
6. Filkov, A.I.; Duff, T.J.; Penman, T.D. Frequency of Dynamic Fire Behaviours in Australian Forest Environments. *Fire* **2020**, *3*, 1. [CrossRef]
7. Thomas, C.M.; Sharples, J.J.; Evans, J.P. Modelling the dynamic behaviour of junction fires with a coupled atmosphere–fire model. *Int. J. Wildland Fire* **2017**, *26*, 331–344. [CrossRef]
8. Lahaye, S.; Sharples, J.; Matthews, S.; Heemstra, S.; Price, O.; Badlan, R. How do weather and terrain contribute to firefighter entrapments in Australia? *Int. J. Wildland Fire* **2018**, *27*, 85–98. [CrossRef]
9. Bishop, S.R.; Drysdale, D. Fires in compartments: The phenomenon of flashover. *Philos. Trans. R. Soc. Lond. Ser. A Math. Phys. Eng. Sci.* **1998**, *356*, 2855–2872. [CrossRef]
10. Drysdale, D. *An Introduction to Fire Dynamics*; John Wiley & Sons, Ltd.: Hoboken, NJ, USA, 2011; pp. 475–526.
11. Vaz, G.; Raposo, J.; Reis, L.; Monteiro, P.; Viegas, D. Rigid Protection System of Infrastructures against Forest Fires. *Fire* **2022**, *5*, 145. [CrossRef]
12. Barbosa, T.F.; Reis, L.; Raposo, J.; Viegas, D.X. A Protection for LPG Domestic Cylinders at Wildland-Urban Interface Fire. *Fire* **2022**, *5*, 63. [CrossRef]
13. Raposo, J.R.N.; Raposo, H.D.N.; Reis, L.; Almeida, E.; Rodrigues, A. Fire in house: Investigation of the outbreak and spread of the fire in a countryside house. *Proc. Inst. Civ. Eng.-Forensic Eng.* **2024**, *178*, 1–7. [CrossRef]
14. Madrzykowski, D. Fire Dynamics: The Science of Fire Fighting. *Int. Fire Serv. J. Leadersh. Manag.* **2013**, *7*, 7–15.
15. Cruz, A.C.; Correa, R.E. *Forest Management: Technology, Practices and Impact*; Nova Science Publishers Inc.: New York, NY, USA, 2012.
16. Werth, P.A.; Potter, B.E.; Clements, C.B.; Finney, M.A.; Goodrick, S.L.; Alexander, M.E.; Cruz, M.G.; Forthofer, J.A.; McAllister, S.S. *Synthesis of Knowledge of Extreme Fire Behavior: Volume I for Fire Managers*; U.S. Department of Agriculture, Forest Service: Portland, OR, USA, 2011.
17. Dold, J.W. Flow attachment in eruptive fire growth. In Proceedings of the 6th International Conference on Forest Fire Research, Coimbra, Portugal, 18–19 November 2010.
18. Byram, G.M. Combustion of Forest Fuels. In *Forest Fire: Control and Use*; Davis, K.P., Ed.; McGraw-Hill: New York, NY, USA, 1959.
19. Morvan, D. Physical Phenomena and Length Scales Governing the Behaviour of Wildfires: A Case for Physical Modelling. *Fire Technol.* **2011**, *47*, 437–460. [CrossRef]
20. Modarres, M. *Experimental and Numerical Analysis of Fire Behaviour in Typical Fuels at the Wildland-Urban Interface*; ADAI: Coimbra, Portugal, 2025.
21. Fernandes, P. FIRE PARADOX: A European initiative on Integrated Wildland Fire Management. In Proceedings of the Fire, Environment and Society, from Research into Practice—The International Bushfire Conference Incorporating the 15th AFAC Conference, Adelaide, SA, Australia, 1–3 September 2008.
22. Ribeiro, C.; Reis, L.; Raposo, J.; Rodrigues, A.; Viegas, D.X.; Sharples, J. Interaction between two parallel fire fronts under different wind conditions. *Int. J. Wildland Fire* **2022**, *31*, 492–506. [CrossRef]
23. Dlugogorski, B.; Hirunpraditkoon, S.; Kennedy, E. Ignition Temperature and Surface Emissivity of Heterogeneous Loosely Packed Materials from Pyrometric Measurements. *Fire Saf. Sci.* **2014**, *11*, 262–275. [CrossRef]
24. Ytong Parameters. 2025. Available online: https://topeca.pt/Imgs/produtos/004/37/50/ficheiros_pt/Ficha_tecnica_bloco_ytong_550_kg.pdf (accessed on 19 September 2025).
25. *EN 771-4:2011+A1:2015*; Specification for Masonry Units—Part 4: Autoclaved Aerated Concrete Masonry Units; German Version. German Institute for Standardisation: Berlin, Germany, 2015.

26. Cruz, M.G. *Guia Fotográfico para Identificação de Combustíveis Florestais—Região Centro de Portugal*; Centro de Estudos sobre Incêndios Florestais, Associação para o Desenvolvimento da Aerodinâmica Industrial (ADAI), Universidade de Coimbra: Coimbra, Portugal, 2005.
27. Martins Fernandes, P.A. Fire spread prediction in shrub fuels in Portugal. *For. Ecol. Manag.* **2001**, *144*, 67–74. [CrossRef]
28. Alves, D.; Almeida, M.; Reis, L.; Raposo, J.; Viegas, D.X. The Role of Field Measurements of Fine Dead Fuel Moisture Content in the Canadian Fire Weather Index System—A Study Case in the Central Region of Portugal. *Forests* **2024**, *15*, 1429. [CrossRef]
29. Viegas, D.X.F.C.; Raposo, J.R.N.; Ribeiro, C.F.M.; Reis, L.C.D.; Abouali, A.; Viegas, C.X.P. On the non-monotonic behaviour of fire spread. *Int. J. Wildland Fire* **2021**, *30*, 702–719. [CrossRef]
30. Finney, M.A. *FARSITE: Fire Area Simulator—Model Development and Evaluation*; USDA Forest Service, Rocky Mountain Research Station: Ogden, UT, USA, 1998.
31. Viegas, D.X.; Pita, L.P. Fire spread in canyons. *Int. J. Wildland Fire* **2004**, *13*, 253–274. [CrossRef]
32. Fernandes, P.M.; Cruz, M.G. Plant flammability experiments offer limited insight into vegetation–fire dynamics interactions. *New Phytol.* **2012**, *194*, 606–609. [CrossRef]
33. Catchpole, E.A.; Catchpole, W.R.; Viney, N.R.; McCaw, W.L.; Marsden-Smedley, J.B. Estimating fuel response time and predicting fuel moisture content from field data. *Int. J. Wildland Fire* **2001**, *10*, 215–222. [CrossRef]
34. Àgueda, A.; Pastor, E.; Pérez, Y.; Viegas, D.X.; Planas, E. Fire intensity reduction in straw fuel beds treated with a long-term retardant. *Fire Saf. J.* **2011**, *46*, 41–47. [CrossRef]
35. Viegas, D.X.; Neto, L.P.C. Wall Shear-Stress as a Parameter to Correlate the Rate of Spread of a Wind Induced Forest Fire. *Int. J. Wildland Fire* **1991**, *1*, 177–188. [CrossRef]
36. Alexander, M.E.; Cruz, M.G. Assessing the effect of foliar moisture on the spread rate of crown fires. *Int. J. Wildland Fire* **2012**, *22*, 415–427. [CrossRef]
37. Lopes, S.; Viegas, D.; Lemos, L.; Viegas, M. Equilibrium moisture content and timelag of dead Pinus pinaster needles. *Int. J. Wildland Fire* **2014**, *23*, 721–732. [CrossRef]
38. Rossi, J.L.; Chatelon, F.J.; Marcelli, T. Fire Intensity. In *Encyclopedia of Wildfires and Wildland-Urban Interface (WUI) Fires*; Manzello, S.L., Ed.; Springer International Publishing: Cham, Switzerland, 2018; pp. 1–6.
39. Weise, D.R.; Biging, G.S. Effects of wind velocity and slope on flame properties. *Can. J. For. Res.* **1996**, *26*, 1849–1858. [CrossRef]
40. Li, H.; Liu, N.; Xie, X.; Zhang, L.; Yuan, X.; He, Q.; Viegas, D.X. Effect of Fuel Bed Width on Upslope Fire Spread: An Experimental Study. *Fire Technol.* **2021**, *57*, 1063–1076. [CrossRef]
41. Grumstrup, T.; McAllister, S.; Finney, M. Qualitative flow visualization of flame attachment on slopes. In Proceedings of the 10th U.S. National Combustion Meeting Organized by the Eastern States Section of the Combustion Institute, College Park, MD, USA, 23–26 April 2017.
42. Campbell-Lochrie, Z.; Walker-Ravena, C.; Gallagher, M.; Skowronski, N.; Mueller, E.; Hadden, R. Effect of Fuel Bed Structure on the Controlling Heat Transfer Mechanisms in Quiescent Porous Flame Spread. In *Advances in Forest Fire Research 2022, Proceedings of the IX International Conference on Forest Fire Research, Coimbra, Portugal, 11–18 November 2022*; Viegas, D.X., Ribeiro, L.M., Eds.; Imprensa da Universidade de Coimbra: Coimbra, Portugal, 2022; pp. 1443–1448.
43. Wotton, B.M.; McAlpine, R.S.; Hobbs, M.W. The effect of fire front width on surface fire behaviour. *Int. J. Wildland Fire* **2000**, *9*, 247–253. [CrossRef]
44. Cheney, N.; Gould, J.; Catchpole, W. Prediction of Fire Spread in Grasslands. *Int. J. Wildland Fire* **1998**, *8*, 1–13. [CrossRef]
45. Rossa, C.G.; Fernandes, P.M. An Empirical Model for the Effect of Wind on Fire Spread Rate. *Fire* **2018**, *1*, 31. [CrossRef]
46. Drysdale, D.D.; Macmillan, A.J.R.; Shilitto, D. The King's Cross fire: Experimental verification of the 'Trench effect'. *Fire Saf. J.* **1992**, *18*, 75–82. [CrossRef]
47. Sharples, J.; Gill, A.M.; Dold, J.W. The trench effect and eruptive wildfires: Lessons from the King's Cross Underground disaster. In Proceedings of the Australian Fire and Emergency Service Authorities Council 2010 Conference, Darwin, Australia, 10 September 2010.
48. Cruz, M.G.; Sullivan, A.L.; Gould, J.S. The effect of fuel bed height in grass fire spread: Addressing the findings and recommendations of Moinuddin et al. (2018). *Int. J. Wildland Fire* **2020**, *30*, 215–220. [CrossRef]

Disclaimer/Publisher's Note: The statements, opinions and data contained in all publications are solely those of the individual author(s) and contributor(s) and not of MDPI and/or the editor(s). MDPI and/or the editor(s) disclaim responsibility for any injury to people or property resulting from any ideas, methods, instructions or products referred to in the content.